

Adsorption and enzymatic cleavage of osteopontin at interfaces with different surface chemistries

Jenny Malmström^{a)} and Stepan Shipovskov
Interdisciplinary Nanoscience Center (iNANO), University of Aarhus, 8000 Denmark

Brian Christensen and Esben S. Sørensen
Department of Molecular Biology, Protein Chemistry Laboratory, University of Aarhus, 8000 Denmark

Peter Kingshott and Duncan S. Sutherland^{b)}
Interdisciplinary Nanoscience Center (iNANO), University of Aarhus, 8000 Denmark

(Received 4 June 2009; accepted 30 June 2009; published 21 August 2009)

Osteopontin is a highly charged glycoprotein present in the extra cellular matrix of a wide range of tissues. It is, in particular, relevant for biomaterials through its role in mineralized tissue remodeling. The adsorption and enzymatic cleavage of osteopontin at four different surface chemistries (methyl-, carboxylic-, and amine-terminated alkanethiol self-assembled monolayers and bare gold) have been studied utilizing a combination of the quartz crystal microbalance with dissipation and surface plasmon resonance. Full length bovine milk osteopontin was used which is well characterized with respect to post-translational modifications. Osteopontin adsorbed at all the surfaces formed thin (~2–5 nm) hydrated layers with the highest amount of protein and the highest density layers observed at the hydrophobic surface. Less protein and a higher level of hydration was observed at the polar surfaces with the highest level of hydration being observed at the gold surface. The energy dissipation of these thin films (as measured by the $\Delta D/\Delta F$ value) was altered at the different surface chemistries and interestingly a higher dissipation correlated with a higher density. Thrombin was able to bind and cleave the surface bound osteopontin at the hydrophobic surface. The altered levels of osteopontin binding, hydration of the layer, and susceptibility to thrombin cleavage suggest that osteopontin adopts different conformations and/or orientations at the different material surfaces.

© 2009 American Vacuum Society. [DOI: 10.1116/1.3187529]

I. INTRODUCTION

Synthetic materials are widely used for biomedical application and the interactions between the material interface and tissue components are critical for determining the biological outcome of the medical device. Immediately on contacting a physiological fluid, biomaterial surfaces interact with the complex mixture of macromolecules which contains proteins, carbohydrates, and lipids.¹ These biomolecules form a hydrated layer, coating the surface and modifying the tissue-material interface. Adsorbed proteins within the layer mediate the subsequent interactions with cells and not only the type of protein present but also the amount, orientation, and conformation play a vital role for the future of the biomaterial.² As a result, considerable efforts are set into understanding and controlling the interaction of proteins with interfaces. The extracellular matrix surrounding a cell in an *in vivo* environment is remodeled by the release of extracellular components and the action of local specific enzymatic processes.³ At a biomaterial surface the adsorbed proteins within the hydrated cell-mediating layer are also susceptible to modification through for example enzymatic modification. A range of complementary surface sensitive analytical techniques has been developed that allows the interaction of biomolecules adsorbing or adsorbed at a liquid-solid interface to

be studied. Examples include the quartz crystal microbalance with dissipation (QCM-D), ellipsometry, optical waveguide light mode spectroscopy, and surface plasmon resonance (SPR). These techniques can quantify the amounts of protein adsorbing to interfaces,⁴ the viscoelastic properties, and hydration state of the layers⁵ and subsequent molecular interactions within the layer, such as ligand/substrate binding,⁴ conformational change,⁶ or subsequent enzymatic modification.⁷

Osteopontin (OPN) is a highly phosphorylated glycoprotein that is present in the extracellular matrix of a variety of tissues.⁸ OPN can bind to cells via the CD44 receptor and through a arginine-glycine-aspartic acid (RGD) cell adhesive sequence that interacts with integrin receptors in the cell membrane. The RGD sequence has been shown to mediate cell adhesion in a large number of cell types.⁹ OPN has been shown to play a role in the formation and remodeling of mineralized tissue as well as in inflammation and immune responses.⁸ OPN is widely altered via post-translational modifications (PTMs).^{10–13} These PTMs (such as phosphorylation, glycosylation, and proteolytic processing) are highly cell specific, reflecting the diverse functions of OPN in different tissues.¹⁰ OPN belongs to a group of proteins which are only partially structured in the native unbound state but which have been suggested to adopt specific conformations on ligand binding.¹⁴ OPN is highly relevant as a protein ad-

^{a)}Electronic mail: jennym@inano.dk

^{b)}Electronic mail: duncan@inano.dk

sorbed to biomaterial surfaces as it controls many aspects of cell behavior⁸ and is implicated in mineralization, inflammation, and the immune response.

OPN is susceptible to enzymatic cleavage by thrombin, at a site close to the RGD sequence. Upon cleavage by thrombin the conformation around the RGD site may change, exposing both this and a cryptic integrin binding site (serine-valine-valine-tyrosine-glycine-leucine-arginine in human OPN). A variety of human cell lines has been shown to attach and spread better on thrombin cleaved OPN than on full length OPN.¹⁵ *In vivo*, thrombin cleaved OPN exists together with the full length protein.¹⁵

In contrast to other plasma proteins such as fibronectin, collagen, and fibrinogen, the interactions of OPN in a biomaterial context have been relatively little studied. The high degree of diversity within OPNs derived from different tissues, in particular, relating to the number and location of PTMs and the level of enzymatic modifications makes the source of OPN a key issue.⁸ One recent study utilizing recombinant mouse OPN showed a differential ability of the protein to support cell adhesion when adsorbed at different surface chemistries.¹⁶ Enhanced cell adhesion was shown on amine-terminated self-assembled monolayers (SAMs), compared to layers terminated by $-OH$, $-COOH$, and $-CH_3$.¹⁶ OPN adsorption and function have also been characterized when adsorbed to collagen I (Ref. 17) and to polymer surfaces.¹⁸ Furthermore, OPN with different degrees of phosphorylation has been shown to support cell adhesion of different cell types to different degrees¹⁰ and polymeric OPN was shown to mediate a higher degree of cell adhesion of a human colon carcinoma cell line, possibly due to exposure of a cryptic epitope for integrin binding.¹⁹ These facts indicate that the combination of surface chemistry, phosphorylation of OPN, and cell type may all be involved in mediating a highly specific cell response.

This study focuses on developing an understanding of the adsorption and functional behavior of full length OPN at different surface chemistries. OPN from bovine milk exhibits a high degree of phosphorylation and has been well characterized with respect to the post-translational modifications.¹² A combination of QCM-D and SPR has been used to gain information about how this highly phosphorylated variant of OPN interacts with various surface chemistries. Alkanethiol self-assembled monolayers on gold are utilized as well defined surface chemistries of hydrophobic ($-CH_3$ terminated thiol), hydrophilic negatively charged ($-COOH$ terminated thiol), hydrophilic positively charged ($-NH_2$ terminated thiol), and a metallic character (bare gold). The adsorption of OPN at these different surfaces and the adsorbed layer properties in terms of water content and thickness was characterized. In addition the susceptibility of the adsorbed protein layers to enzymatic cleavage by thrombin was used as a specific indicator of availability of a specific binding site and correlated with the physical properties of the layers.

II. EXPERIMENTAL METHODS

A. Materials

Buffers were prepared with MQ water (MilliQ Gradient, Millipore) and filtered through a $0.2\ \mu\text{m}$ pore filter and degassed by the use of sonicator prior to use. The buffer used was HEPES 10 mM (2-[4-(2-hydroxyethyl)-1-piperazinyl] ethanesulfonic acid) with 150 mM NaCl, 9 mM CaCl_2 at pH 7.4. Calcium was present in the buffer to mimic the *in vivo* situation for this calcium binding protein.

Bovine serum albumin (BSA) was purchased from Sigma-Aldrich (cell culture tested $\geq 96\%$ purity). Thrombin protease was purchased from Amersham Biosciences and thrombin inhibitor PPACK II from Calbiochem. OPN was purified from bovine milk essentially as described in Ref. 20. For extra high purity and to remove N-terminal OPN fragments naturally occurring in the milk, an additional step of size exclusion chromatography was performed. The homogeneity and purity (+98%) of the OPN was verified by SDS-PAGE, reverse-phase HPLC, and N-terminal amino acid sequencing.

Thrombin protease was reconstituted by adding ice cold phosphate buffered saline to the thrombin powder directly from the freezer to give a final concentration of 1 U/ml. The thrombin solution was aliquoted and frozen immediately at $-50\ ^\circ\text{C}$. Aliquots were defrosted at $4\ ^\circ\text{C}$ before use and diluted with HEPES buffer to the desired concentration. PPACK II was dissolved in MQ water to a final concentration of 10 mg/ml, aliquoted and frozen at $-20\ ^\circ\text{C}$. Upon use, aliquots were defrosted at $4\ ^\circ\text{C}$ and further diluted in HEPES buffer before added to thrombin samples in a 15 molar excess prior to use in experiments. PPACK II inactivated thrombin is referred to as I thrombin.

B. Substrates

QCM-D crystals, AT-cut quartz crystals with a fundamental resonance frequency of ~ 5 MHz, were purchased from Q-Sense AB (Gothenburg, Sweden) with bare gold electrodes (QSX 301), SPR chips (SIA-Au) were purchased from GE healthcare and pre-cut silicon wafers were purchased from Litcon AB (Gothenburg, Sweden) and coated by 1 nm Ti and 20 nm Au 1 nm Ti (rf magnetron sputtering (home-made), 2×10^{-3} mbar argon pressure, Ti deposition rate of 1 nm/s ($6.45\ \text{W}/\text{cm}^2$), Au deposition rate $2.2\ \text{nm}/\text{s}$ ($2.5\ \text{W}/\text{cm}^2$). All QCM-D and SPR surfaces were treated with TL1 clean 20 min before use (1:1:5 volume ratio $\text{H}_2\text{O}_2:\text{NH}_4:\text{H}_2\text{O}$, $70\text{--}80\ ^\circ\text{C}$) followed by thorough rinsing with MQ water. Gold coated wafers were cleaned by UV/ozone for 1 h prior to use followed by immersing in MQ water for 1 h after UV/ozone treatment to allow for the Au_2O_3 formed²¹ to be reduced back to Au^0 . Some gold surfaces were modified by the assembly of alkanethiols (methyl terminated $\text{C}_{18}\text{H}_{38}\text{S}$, Sigma-Aldrich, carboxy-terminated thiol $\text{HSC}_{15}\text{H}_{30}\text{COOH}$, and amino-terminated $\text{HSC}_{11}\text{H}_{22}\text{NH}_2$, Prochimia, Poland). Thiolation was performed in ethanol (p.a. grade, Merck) for a minimum of 12 h for the methyl terminated thiol (35 mM) and 24–48 h for the

hydrophilic thiols (2 mM). After the assembly the surfaces were sonicated in ethanol (10 min for methyl terminated and 3 min for hydrophilic thiols) to remove unbound thiols, followed by sonication for 3 min in MQ water and subsequent drying under a stream of nitrogen. Substrate chemistry before and after modification was characterized by x-ray photoelectron spectroscopy and advancing water contact angle goniometry (sessile drop). X-ray photoelectron spectroscopy (XPS) spectra showed oriented self-assembled monolayers with the expected surface functional groups (see table S2 in the supplementary information).²² The films formed from amine-terminated thiols showed in addition to the expected atomic constituents also some oxygen, probably indicating a less well ordered thiol layer resulting from oxidation of some of the sulfur groups and/or water coordinated to the amine group. The formation of high quality amino-terminated alkanethiol films has previously been reported to be difficult.²³

C. QCM-D

The quartz crystal microbalance is a sensitive weighing device that can measure mass changes in the nanogram range. In the QCM-D technique,²⁴ the damping of the crystal oscillation (the dissipation factor) is measured in addition to the frequency shift allowing to determine the viscoelastic properties of the layer. For thin and rigid layers the mass adsorbed to the sensor can be calculated using the Sauerbrey equation²⁵ and the mass derived from QCM-D data includes any water coupled to and in the layer.⁵ The measurements were performed with a Q-sense E4 system from Q-Sense AB (Gothenburg, Sweden) where the resonance frequency and the 3rd–13th overtones of the sensor were recorded simultaneously with the damping of the crystal, i.e., the dissipation factor. Each experiment was run in batch mode with pumping of liquid through the sensor when rinsing or exchanging buffers.

For each protein addition, approximately 0.5 ml of liquid was pumped to the sensor using a flow rate of 0.1 ml/min. Thereafter the pump was stopped and the protein adsorption was allowed to continue under static conditions for the remainder of the adsorption step. This protocol was used as a compromise between avoiding depletion effects and limiting the amounts of protein required. The majority of the binding (>90%) occurs during the first 5 min so that the experimental conditions reflect flow conditions. After a stable base line was accomplished, an OPN solution of 20 $\mu\text{g}/\text{ml}$ was introduced and allowed to adsorb to the surface for 1 h in HEPES buffer. Then the surfaces were blocked with BSA 1 mg/ml, 30 min followed by the introduction of thrombin (13 U/ml) or thrombin at the same concentration inhibited by PPACK II (PPACK II incubated with thrombin in 15 molar excess for 10 min prior introduction in the instrument) for 1 h. The chamber was rinsed for 15 min with HEPES buffer after each step.

D. SPR

Surface plasmon resonance is an optical technique which utilizes surface plasmon polariton excitations to sense the local refractive index change in the liquid close to the gold surface. If biomolecules are adsorbed on a surface, they replace the buffer next to the surface, and the change in refractive index can be converted to adsorbed (dry or optical) mass.²⁶

Measurements were performed with a Biacore X system from Biacore AB (Uppsala, Sweden). A flow rate of 5 $\mu\text{l}/\text{min}$ was used, and a stable base line was awaited before adsorption. The procedure followed that of a QCM-D experiment with the same buffers and chemicals with shorter contact time between surface and protein solutions (30 min) due to instrument configurations but, in general, the adsorption finished faster for the SPR measurements than the QCM-D experiments due to the flow versus static conditions.

Figure 4 has been subjected to a base line correction to display the data better. 5–10 min of data previous to the injection was used to fit a line using linear regression (MICROSOFT EXCEL).

E. SDS-PAGE electrophoresis

SDS-PAGE electrophoresis was performed using the Invitrogen Power ease 500 fitted with Novex minicell. Samples were loaded on a NuPAGE[®] 4%–12% Bis-Tris gel (Invitrogen) and run at 200 V for 40 min with NuPAGE[®] MOPS SDS running buffer. Samples were prepared for loading by adding a buffered solution containing glycerol, SDS, DTT, and bromphenol blue, followed by immersing the samples in a water bath, $\sim 90^\circ\text{C}$, for 10 min. SeeBlue[®] Plus2 Prestained standard (Invitrogen) was loaded on the gel for size comparison. After the gel was run it was washed twice with MQ water, stained with Simply blue safe stain (Invitrogen) for 1 h and rinsed repeatedly with MQ water. Finally, the gel was dried out using DryEase minigel drying system (Invitrogen).

F. Statistics

The unequal variance *t* test was used for the statistical analysis of the data.²⁷ In general the unequal variance *t* test was performed on the data sets with EXCEL. The sample size for the analysis of OPN and BSA layers was eight for QCM-D and SPR data (for SPR these eight data points are constituted by four independent experiments with data from two flow channels in each). For the calculation of the density the error was estimated by calculating the density for all possible combinations of dry and wet mass for each surface chemistry, giving rise to 64 density values for each group. The mean was calculated from these 64 values while the *P* value was calculated following the approach presented by Ruxton *et al.*²⁷ using the original sample size of eight when calculating the degrees of freedom. Probability values of ≤ 0.05 were considered to indicate significant differences. The results are expressed as mean \pm standard deviation and

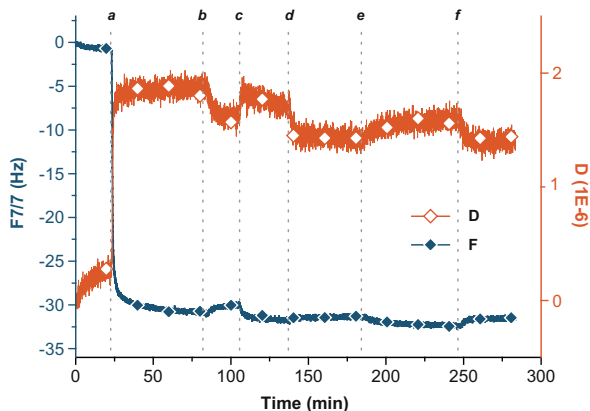


Fig. 1. (Color online) Typical QCM-D graph for an experiment on a gold surface showing the (a) OPN adsorption followed by (b) buffer rinse blocking with (c) BSA, (d) buffer rinse, (e) thrombin, and (f) a final rinse. Frequency and dissipation displayed.

significant differences are indicated in the text. Contact angle measurements were done with a sample size of four.

III. RESULTS

We have monitored OPN adsorption to four different surface chemistries, and observe different situations on each of these surfaces. Differences range from the amount of adsorbed protein to water content of the layer, stability of the OPN on the surface and accessibility to thrombin.

The advancing contact angle measurements ($n=4$) showed hydrophilic surface properties for the carboxy-terminated ($20 \pm 2^\circ$), amino-terminated ($40 \pm 4^\circ$), and gold layers ($37 \pm 2^\circ$) and hydrophobic surface properties for the methyl terminated layers ($106 \pm 1^\circ$).

Figure 1 is showing a typical QCM-D graph for the OPN adsorption, blocking with BSA and subsequent exposure to thrombin on a gold surface. The data outlining the frequency and dissipation changes measured by the QCM-D technique for adsorption of OPN at the different surface chemistries are tabulated in the supplementary information. In Table I the data from the OPN and BSA part of the experiment, including both QCM-D and SPR (the thrombin part will be evaluated later in the text and in Fig. 4), are displayed as adsorbed mass per unit area. Significant differences for the wet mass (including $\Delta D/\Delta F$ values) are observed for all comparisons except amine versus carboxylic. The calculated densities are

all significantly different except for the amine versus carboxylic and carboxylic versus gold. The dry mass exhibits fewer significant differences with only hydrophobic versus the charged surfaces being significantly different. The mass from QCM-D includes both the adsorbed biomolecules and any water coupled in or to the layer, whereas SPR gives the optical or dry mass. The mass from the QCM-D measurements were calculated using the Sauerbrey equation,²⁵

$$\Delta m = -\frac{C\Delta f}{n}, \quad (1)$$

where C is the mass-sensitivity constant ($C = 17.7 \text{ ng Hz}^{-1} \text{ cm}^{-2}$ for 5 MHz resonance frequency), n is the overtone number, Δm (ng/cm^2) is the adsorbed mass per unit area, and Δf (Hz) is the frequency shift. The Sauerbrey equation is valid for thin and rigid layer and is a good approximation for our data in this case. The mass from the SPR measurements was calculated using the following formula:²⁸

$$\Delta m = \frac{l_{\text{decay}}}{2} \frac{dc}{dn} \frac{dn}{d\Theta} \Delta\Theta = C_{\text{SPR}} \Delta\text{RU}, \quad (2)$$

where l_{decay} (m) is the decay length the evanescent field [308 nm for instrumental wavelength of 765 nm (Ref. 29)], dc/dn (kg/m^3) is the inverse index increment for the adsorbed molecular layer (0.180 g/ml for most proteins⁴), $\Delta\Theta$ (deg) is the change in resonant angle, and we calibrated $dn/d\Theta$ for the instrument using solutions of different concentrations of glucose. For our instrumental setup with the Biacore X C_{SPR} was calibrated to be 0.082 ng/cm^2 for protein adsorption directly onto the gold surface. ΔRU is the difference in response units after and before the adsorption and it is directly correlated with the change in SPR angle (1000 RU correspond to $\Delta\Theta \sim 0.1^\circ$).³⁰

A combination of optical techniques with QCM can be used to quantify the properties of adsorbed organic layers, such as polyelectrolyte layers,³¹ proteins,⁴ and lipids.²⁸ The combination of QCM-D and SPR allows for calculating the water content of the adsorbed biomolecular layer. The densities for the OPN layers at different surface chemistries are displayed in Table I and were calculated according to Eq. (3), where ρ_{prot} was assumed to be 1325 kg/m^3 ,³²

$$\rho_{\text{layer}} = \frac{m_{\text{QCM}}}{m_{\text{SPR}}/\rho_{\text{prot}} + (m_{\text{QCM}} - m_{\text{SPR}})/\rho_{\text{water}}}. \quad (3)$$

TABLE I. Summary of adsorption data for OPN and following BSA blocking. Wet mass from QCM-D and Dry mass from SPR.

	Sauerbrey ("wet") mass (ng/cm^2)	Dry mass (ng/cm^2)	Density (kg/m^3)	$\Delta D/\Delta F$ (10^{-6} Hz^{-1})
Au: OPN adsorption	498 ± 32	78 ± 12	1040 ± 6.7	$0.0477 \pm 0.002 \text{ 05}$
Au: BSA	19 ± 13	25 ± 7.7		
Hydrophobic: OPN adsorption	257 ± 116	117 ± 53	1151 ± 86	0.113 ± 0.0223
Hydrophobic: BSA	250 ± 45	38 ± 13		
Carboxylic: OPN adsorption	361 ± 43	69 ± 17	1050 ± 14	$0.0585 \pm 0.008 \text{ 96}$
Carboxylic: BSA	86 ± 19	3.9 ± 13		
Amine: OPN adsorption	361 ± 15	71 ± 12	1051 ± 8.9	$0.0572 \pm 0.008 \text{ 96}$
Amine: BSA	17 ± 13	0 ± 25		

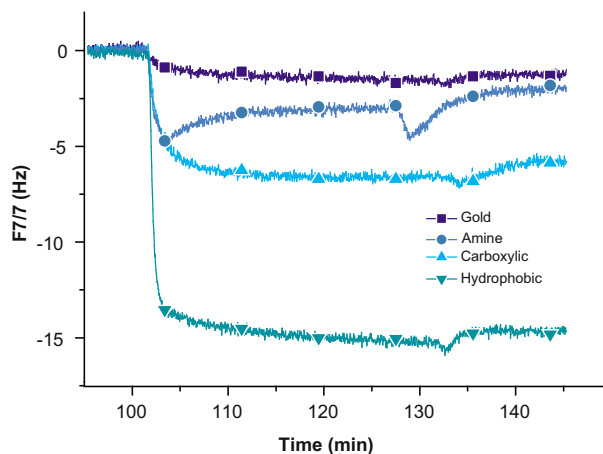


FIG. 2. (Color online) Examples of QCM-D graphs (frequency only) showing the BSA adsorption at the four different surface chemistries. Note that the graphs are offset to start at zero frequency after the OPN adsorption for easy comparison. To see how much OPN that adsorbed on each surface chemistry see Fig. 1 or Table I.

As can be seen in Table I, the density of the OPN layers differs between the different surfaces. A considerably higher density layer is observed at the hydrophobic surface ($\sim 1150 \text{ kg/m}^3$), whereas both the charged surfaces (amine and carboxylic) show a similar density ($\sim 1050 \text{ kg/m}^3$). The lowest density and consequently the highest water content was seen on the gold surface ($\sim 1040 \text{ kg/m}^3$). The absolute calculated values for layer densities are dependent on the generic values for dc/dn of the adsorbed molecular layer and ρ_{prot} (density of dry protein). These generic values may not be perfectly correct for any given case but is not expected to be a major source of error and will not affect the differences between the surface chemistries studied here.

The QCM-D technique provides information both on the additional mass adsorbed at the sensor surface (through the frequency shift upon protein binding) and on the energy dissipation of the adsorbed layer. The energy dissipation shift increases as the frequency shift decreases (as seen in Fig. 1) as each material accumulates at the interface, thus the dissipation shift per unit frequency shift is often used as an indicator of the energy dissipation. The $\Delta D/\Delta F$ values after rinsing for the OPN layers adsorbed at the different surface chemistries are for the amine-terminated surface 0.057 ± 0.003 , for the carboxyl-terminated surface 0.058 ± 0.009 , for the methyl terminated surface 0.113 ± 0.022 , and for the gold surface 0.048 ± 0.002 .

The surfaces were blocked with BSA after OPN adsorption to hinder unspecific binding of thrombin to the underlying substrate. The BSA adsorption itself can reveal extra information about the coverage and strength of interaction of OPN with the different surface chemistries.

In Fig. 2 it can be seen that there are large variations in the level of binding of BSA. The hydrophobic surface where the least OPN binding is observed with QCM-D corresponds to the largest BSA binding (see Fig. 1 or Table I). Significant variation in the BSA data resulting from SPR makes it difficult to conclude much from these data; however the highest

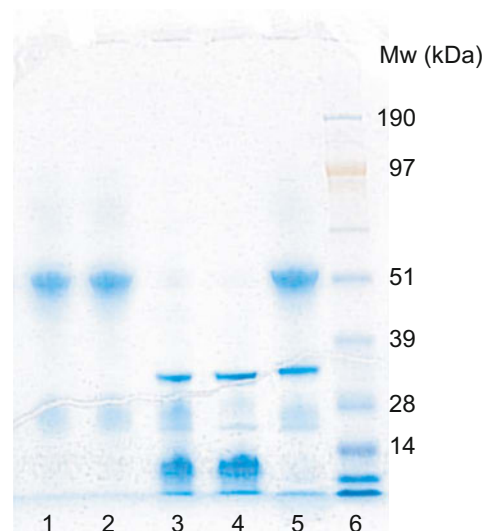


FIG. 3. (Color online) SDS-PAGE gel showing full length OPN being cleaved by thrombin, and how PPACK II efficiently inhibits thrombin. The following conditions run: (1) OPN 1 mg/ml; (2) OPN 1 mg/ml incubated 30 min at RT; (3) OPN 1 mg/ml+thrombin, 0.2 mg/ml incubated 10 min at RT; (4) OPN 1 mg/ml+thrombin, 0.2 mg/ml incubated 30 min at RT; (5) OPN 1 mg/ml+thrombin, 0.2 mg/ml+PPACK II, incubated 30 min at RT; (6) See Blue standard.

binding was observed for the hydrophobic surface in agreement with the QCM-D data. Interestingly the kinetics of the BSA adsorption shows a different behavior on the amine surface. The shape of the graph, with an increase in resonance frequency seen after the initial drop in frequency, may indicate both that BSA is binding to the surface in significant amounts and that some other process leading to loss of material is also occurring. The second dip in the graphs in Fig. 2 corresponds to when the surface is rinsed with buffer after BSA adsorption, and thus “fresh” BSA remaining in the tubing, is again flowed over the sensor surface giving a small increase in binding before the buffer reaches the sensors and some desorption appears to start to occur. This is a common scenario seen with this instrumental setup.

We aimed to use the accessibility of OPN to thrombin as a tool to gauge functionality of the protein since it has previously been shown to be advantageous for cells to bind to the cleaved form of the protein. Additionally, since the thrombin cleavage site is in close proximity to the RGD cell binding site, the binding of thrombin to OPN could well correlate to RGD availability. We have both observed the interaction of active thrombin and thrombin inhibited with PPACK (I thrombin) to OPN. The gel in Fig. 3 clearly shows that thrombin is able to cleave OPN (compare lane 2 with lane 4) and that PPACK II is able to inhibit this thrombin cleavage (compare lane 4 with lane 5). The upper band seen in lanes 1, 2, and 5 at $\sim 51 \text{ kDa}$ corresponds to full length OPN; the lower intense band in lanes 3–5 at $\sim 35 \text{ kDa}$ corresponds to thrombin. The migration of the highly phosphorylated OPN is as expected not well represented by the protein standard (due to poorly pairing with the SDS) but can be

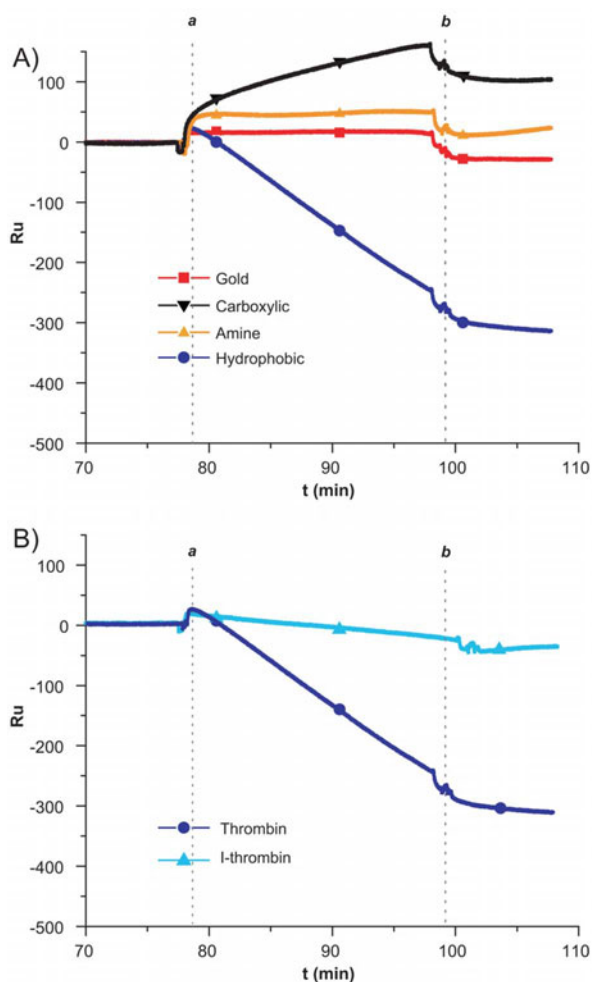


FIG. 4. (Color online) Examples of SPR graphs showing (a) thrombin interacting with surface adsorbed OPN for all surface chemistries. (b) The difference between active thrombin and thrombin inhibited by PPACK II for the hydrophobic surface. *a* indicates point of injection of OPN and *b* indicates the start of rinsing with buffer. Each curve has been offset to start at zero Ru and corrected for baseline drift by subtracting the drift for the time before the injection of thrombin or thrombin inhibited by PPACK II.

used to investigate its purity and cleavage (the mass of the bovine milk OPN used here is ~ 33.9 kDa as determined by MALDI MS).

SPR measurements were used to study the interaction of thrombin with the OPN layers at the different surface chemistries. In our case we observed three different scenarios [Fig. 4(a), the data is also available in original form prior to baseline correction is supplementary information]²². On the hydrophobic surface a linear reduction in mass is seen during the thrombin exposure step. The rate of removal of material from the surface is seen to be greatly reduced by inhibition of the thrombin with PPACK II [shown in Fig. 4(b)], which indicates that the mass leaving the surface results from enzymatic cleavage of OPN by thrombin. On the other surface chemistries no such reduction in mass was observed. However on the carboxylic surface a net increase in mass was observed after the thrombin exposure step. In the raw SPR data we observed drift of the signals which were different in each experiment. We do not fully understand this drift which

is likely to be a combination of machine induced drift and possible desorption of material from the surface. Such effects make a quantification of the enzymatic effect difficult, but to display the data better we have subtracted the drift in the “base line” before the injection of thrombin or thrombin inhibited by PPACK II in Fig. 4. The original data for Fig. 4(a) are available in supplementary information. However a clear qualitative difference is observed in the interaction of thrombin with OPN adsorbed at the different surface chemistries.

We have carried out parallel QCM-D studies for the thrombin step which were however rather inconclusive. We could, in some cases, confirm the enzymatic cleavage at the hydrophobic surfaces (for those cases when a relatively large amount of OPN was adsorbed to the surface), but did not observe significant changes in the mass during thrombin exposure for the other chemistries.

IV. DISCUSSION

The combination of multiple surface analytical techniques can increase the quality of information obtained about surface adsorbed protein layers. Here we utilize the optical technique SPR which measures the surface density of protein in combination with the acoustic technique QCM-D, which gives information on the total mass of the hydrated adsorbed layer. The properties of the adsorbed OPN layers are found to be significantly different at the different surface chemistries studied. The amount of OPN adsorbing at the polar hydrophilic and metal surfaces was found to be relatively similar. Assuming a protein surface packing via random sequential adsorption the adsorbed mass of ~ 75 ng/cm² corresponds to a footprint of ~ 40 nm²/molecule indicating a relatively low surface coverage. OPN is believed to have little structure in solution and may adopt a structure upon ligand binding.¹⁴ The mass adsorbing to the hydrophobic surface chemistry was $\sim 50\%$ larger than the other surfaces (~ 115 ng/cm², see Table I) and with a concomitantly smaller molecular footprint (24 nm²/molecule) although with a substantial variability. The QCM-D measurements show a somewhat different profile with the largest binding observed for the metal surface and the least at the hydrophobic surface. Compared to the polar hydrophilic surfaces the gold surface shows a significantly larger additional binding ($\sim 50\%$) and the hydrophobic surface, a significantly lower binding ($\sim 25\%$). While the SPR technique measures the optical or dry mass of the protein, the QCM-D techniques additionally measure water mass trapped within the protein layer. The differences in the measured signals indicate first that the OPN layers bound at the different surface chemistries include significant amounts of trapped water but also that the level of water bound within the protein layer is related to the surface chemistry. A comparison of the two techniques allows the extraction of the level of hydration. While water makes up $\sim 65\%$ of the OPN layer at the hydrophobic surface, it represents more than $\sim 85\%$ of the films at the polar hydrophilic surfaces and greater than 88% at the metal surface. The level of hydration of a protein film can give some information about the conformation of proteins within

the layer. Adsorbed layers of a number of extracellular matrix proteins have been studied utilizing QCM-D combined with optical techniques (e.g., HSA, IgG, fibronectin, and laminin^{4,29,33,34}). While a general trend is seen with a higher level of hydration for larger proteins, for specific proteins altered levels of hydration have been observed when the protein is adsorbed at different surface chemistries. For one specific protein, the mussel adhesive protein, Höök *et al.*⁵ showed that a low/high density correlated with two different conformations of the protein with the high density state induced by specific cross-linking. The altered level of hydration of proteins at different surface chemistries is thought to indicate altered conformations at the different interfaces. The level of hydration of small proteins has not been extensively studied. The level of hydration that we observe for OPN (~34 kDa) is higher than that observed for somewhat larger globular proteins (e.g., hemoglobin 64.5 kDa gave 43% hydration and HSA 66 kDa gave 44% hydration at a hydrophilic titanium dioxide surface⁴). The relative lack of structure observed for OPN may explain the high levels of hydration compared to these more compact proteins. The two-technique approach also allows the extraction of a thickness for each of the adsorbed protein films by dividing the total Sauerbrey mass (hydrated mass) by the density of the layer and also shows a dependence on the surface chemistries. Our calculations assume a homogenous layer which has recently been shown to lead to an underestimation of the layer thickness, especially in cases of low protein coverage.³⁵ Clearly the density of the layer may not be constant throughout the layer so these numbers represent a characteristic thickness allowing comparison between layers formed at the different interfaces. The thickness of the films are different on the metal, polar, and charged surfaces, respectively, and correlate to the density of the films rather than the total mass with a lowest density (e.g., at the metal surface) giving the thickest film. This means that the gold surface has a thickness of ~5 nm while the thickness is ~3.5 nm on the polar surfaces and ~2 nm on the hydrophobic surface (highest density film). The hydrophobic surface with the smallest molecular footprint gave the thinnest film tells something about the interaction of the protein with the different surface chemistries. While the larger molecular footprint of OPN at the gold and the polar surfaces might suggest an open conformation with multiple contact points to the surface, the relatively thicker films observed suggest less contact between the protein and the surface. OPN at the hydrophilic surfaces may have a more open structure and larger size taking up a greater area on and extending further from the surface. At the hydrophobic surface an altered conformation is suggested with a more compact structure.

The energy dissipation of the OPN films (as quantified by the $\Delta D/\Delta F$ value) at the different surface chemistries measured by the QCM-D showed differences (significant for all but a comparison of the two polar surfaces) and a clear correlation to the density of the films obtained from the combination of QCM-D and SPR. The highest $\Delta D/\Delta F$ value was seen for the hydrophobic surface which showed the highest

density of the adsorbed protein layer. This dissipation value and density of the two polar surfaces was significantly lower than that of the hydrophobic surface and significantly higher than at the gold surface. For thick and highly dissipative films the dissipation is usually interpreted in terms of the viscoelastic properties of the film with higher dissipation and $\Delta D/\Delta F$ correlating to floppier films often including larger amounts of water. The films here are neither thick nor highly dissipative (which is confirmed by our attempts to model the data using the Q-soft tools which did not give good fits—data not shown). For thin protein films, such as here, which are rigidly coupled to the surface, the origin of the dissipation is less clear. While the specific origin of the dissipation is hard to interpret, it does in this case scale with the density and we suggest that the dissipative mechanism may relate to interactions within and between the chains of the protein itself.

During our experiment we exposed the OPN coated substrates to a solution of BSA as part of a blocking step. Interestingly the amount of binding observed in the QCM-D was different at the different surface chemistries. While the profile of the binding (Fig. 2) to the Au, CH₃, and COOH surfaces showed typical binding kinetics, those observed at the amine-terminated surface showed an initial binding kinetics for the first few minutes of exposure to BSA followed apparently by a removal of material from the surface (as seen by an increase in frequency). This profile may be explained by a process where initial binding of BSA to the surface stimulates the release of OPN. Such exchange of proteins has been observed before for larger proteins displacing smaller proteins.³⁶ It is unlikely that Table I reflects the full binding of BSA to these surfaces (SPR shows similar kinetics during the BSA adsorption on the amine surface, data not shown). A removal of OPN from the surface by BSA would suggest that the protein has a relatively weaker interaction with the positively charged amine-terminated surface than with the negatively charged carboxyl-terminated surface, which is somewhat surprising given the large number of negatively charged residues in OPN. Calcium present in the system may contribute to binding at the negatively charged surface through the formation of calcium bridges between negatively charged groups on the protein and materials interface, respectively. We cannot however rule out that the observed effects at the amine-terminated surfaces result from other processes such as structural changes in the layer or a process where BSA binds and then leaves the surface. At the hydrophobic surface the level of binding of BSA was surprisingly large which may indicate either that the OPN layer does not fully cover the surface allowing BSA to bind to the hydrophobic substrate or that the conformation of the adsorbed protein allows BSA to bind to the OPN within the layer or to the surface while compacting an initially spread OPN.

The conformation of a surface bound protein is difficult to study. We have utilized thrombin as a probe of the thrombin cleavage site at Arg147-Ser148 (Ref. 12) to gain information about availability of a specific ligand. It has previously been shown that cleavage of the OPN makes the cell binding site

more available. Therefore, the ability of OPN to regulate cell surface binding in a biologically relevant situation, where enzymes are ubiquitous, may be influenced by the enzymatic cleavage. The difference in level of hydration and thickness of the adsorbed protein film suggests that the conformation of the protein is altered at the different surfaces. We observe significant differences during the interaction with thrombin. OPN at the hydrophobic surface is cleaved by thrombin (control measurements of thrombin on BSA showed no binding of thrombin or loss of mass from the surface—data not shown) leading to loss of mass from the surface, while OPN at the other chemistries was not apparently cleaved. An increase in mass was observed with SPR at the carboxylic surface when OPN was subjected to thrombin. We believe that the carboxylic surface is properly blocked by BSA and expect this mass increase to be due to a specific interaction between the thrombin and the OPN; however we cannot completely rule out contributions from unspecific interactions. This mass increase was not detected using QCM-D and the lack signal compared to the SPR could be explained by alterations within the layer (such as a replacement of water within the layer by protein) since QCM-D mass represents both protein and water coupled within the film. The fact that OPN can be cleaved by thrombin at the hydrophobic surfaces suggests an alternative conformation at this surface, which is also suggested by the denser film and smaller molecular footprint of OPN at this surface chemistry as compared to the other surface chemistries.

The adsorbed OPN layers show significant differences in amount adsorbed, hydration, stability, and availability to be cleaved by thrombin. These differences in layer properties suggest that OPN has adsorbed with differences in orientation and conformation on the different surfaces. OPN is regarded as a poorly structured protein in its native state in solution and is included in the class of intrinsically unstructured proteins that are proposed to adopt specific conformations only upon ligand binding.¹⁴ The lack of structure would imply that the protein, as it comes down to the surface, would more easily interact with materials surfaces in different conformations. The different surface chemistries, which result in distinctly different OPN layers with different properties (both physical and functional), suggest that the surface is able to induce some conformation (or set of conformations) of the protein. For a highly structured protein the modulating effect of the surface is normally rather discussed in terms of the amount to which the native structure is lost through denaturation. Here we may observe surface induced conformation able to modulate the functional properties of the protein. Material surfaces can act as specific ligands for molecule recognition molecules³⁷ and OPN is believed to have specific interactions with calcium phosphate interfaces. However, it is unlikely that OPN forms a specific conformation at the interfaces studied here, but perhaps rather a preferred orientation and availability of specific sites. It is easy to imagine how these differences could carry through to yield different cell responses on the different surfaces, but it is hard to predict exactly how and which surface will give

the most beneficial cell behavior. Obviously more factors play in, what is considered beneficial cell behavior in a certain application for one, but also the cell type may influence the outcome. It has previously been shown that mouse *ras*-transformed fibroblasts adhere strongly to two different sources of OPN with different degrees of PTMs, while human breast cancer cells exhibited a much stronger adhesion to the least phosphorylated OPN.¹⁰ The fact that the cell type is of importance indicates that simply the availability of the RGD sequence is not of sole importance, but that other parts of the protein are also influencing the cell adhesion, with phosphorylations being pointed out as one such important factors.

Liu *et al.*¹⁶ previously explored cell binding to an OPN adsorbed to four surface chemistries, $-\text{CH}_3$, $-\text{OH}$, $-\text{NH}_2$, and $-\text{COOH}$ produced by SAMs on gold. Their study revealed the highest cell adhesion and largest cell area on the $-\text{NH}_2$ surface suggesting that their OPN had a favorable orientation/conformation for adhesion and spreading of their primary endothelial cells (bovine aortic). While there are significant differences in their protein system compared to ours, they utilize a recombinant mouse OPN expressed in a myeloma cell line, a higher protein concentration ($50 \mu\text{g}/\text{ml}$) and using calcium free buffer, the study by Liu *et al.*¹⁶ served as an interesting comparison. Liu *et al.* also saw that an equivalent amount of OPN adsorbing on both charged surface chemistries therefore attribute the difference in cell response to orientation and conformation. They show examples of SPR spectra of the amount of OPN adsorbed to the two charged surfaces (they do not report on the other two surfaces) and find three times as much OPN compared to our experiments. The additional binding was unlikely to be a result purely of the higher concentration of OPN since we have investigated the adsorption isotherm on the amine-terminated surface and found that $20 \mu\text{g}/\text{ml}$ is sufficient to be in the higher part of the isotherm (see supplementary information). We do not believe that the presence of calcium is the critical factor since both we and they observed similar adsorption characteristics to positive and negative surfaces. The profile or level of modification of the particular recombinant mouse OPN used in that study has not been established, whereas the bovine milk OPN used in this study has been comprehensively characterized.¹³ OPN from different tissues and species have different patterns of PTMs,^{10,11,14} which could explain the discrepancy in binding. Our analysis of hydration, stability, and susceptibility for thrombin cleavage provides new information on the effect of surface chemistry. In our case, with our source of OPN, further analysis reveals very little difference between the layers on the two charged surfaces. The stability of the layer is the one factor that we have been able to identify that differs between the two surface chemistries, with the cell response still remaining to be investigated in future studies.

V. CONCLUSIONS

In this study the adsorption of OPN to four different surface chemistries has been carefully investigated. A combina-

tion of surface sensitive techniques (QCM-D and SPR) was used to derive information about the protein layers such as the amount adsorbed and hydration. OPN adsorbed in thin layers with a relatively high degree of hydration on all of the surfaces, with the highest density film on the hydrophobic surface and the lowest density film on the bare gold surface. The OPN films adsorbed at the charged hydrophilic interfaces were similar in both amount and hydration, with the only apparent difference being a less stable OPN layer on the amine surface. OPN adsorbed at the hydrophobic surface was shown to be susceptible to enzymatic cleavage by thrombin, while this effect was not detected for the other surface chemistries. The differences detected in the layer properties suggest that OPN, which is proposed to be relatively unstructured in solution, adopts different conformations and/or orientations at the different surface chemistries. It is likely that the response of cells to surface bound OPN will reflect these differences in conformation/orientation.

ACKNOWLEDGMENT

Part of the funding for this project came from the Danish Research Agency internationalization Grant No. 645-05-0016.

¹B. Kasemo, *Surf. Sci.* **500**, 656 (2002).

²B. G. Keselowsky, D. M. Collard, and A. J. Garcia, *J. Biomed. Mater. Res. Part A* **66A**, 247 (2003).

³A. Page-McCaw, A. J. Ewald, and Z. Werb, *Nat. Rev. Mol. Cell Biol.* **8**, 221 (2007).

⁴F. Hook *et al.*, *Colloids Surf., B* **24**, 155 (2002).

⁵F. Hook, B. Kasemo, T. Nylander, C. Fant, K. Sott, and H. Elwing, *Anal. Chem.* **73**, 5796 (2001).

⁶A. G. Hemmersam, K. Rechendorff, F. Besenbacher, B. Kasemo, and D. S. Sutherland, *J. Phys. Chem. C* **112**, 4180 (2008).

⁷K. M. Evans-Nguyen, R. R. Fuieler, B. D. Fitchett, L. R. Tolles, J. C. Conboy, and M. H. Schoenfish, *Langmuir* **22**, 5115 (2006).

⁸J. Sodek, B. Ganss, and M. D. McKee, *Crit. Rev. Oral Biol. Med.* **11**, 279 (2000).

⁹E. Ruoslahti and M. D. Pierschbacher, *Science* **238**, 491 (1987).

¹⁰B. Christensen, C. C. Kazanecki, T. E. Petersen, S. R. Rittling, D. T. Denhardt, and E. S. Sørensen, *J. Biol. Chem.* **282**, 19463 (2007).

¹¹B. Christensen, M. S. Nielsen, K. F. Haselmann, T. E. Petersen and E. S. Sørensen, *Biochem. J.* **390**, 285 (2005).

¹²E. S. Sorensen, P. Hojrup, and T. E. Petersen, *Protein Sci.* **4**, 2040 (1995).

¹³B. Christensen, T. E. Petersen, and E. S. Sorensen, *Biochem. J.* **411**, 53 (2008).

¹⁴L. W. Fisher, D. A. Torchia, B. Fohr, M. F. Young, and N. S. Fedarko, *Biochem. Biophys. Res. Commun.* **280**, 460 (2001).

¹⁵L. R. Rodrigues, J. A. Teixeira, F. L. Schmitt, M. Paulsson, and H. Lindmark-Månsson, *Cancer Epidemiol. Biomarkers Prev.* **16**, 1087 (2007).

¹⁶L. Y. Liu, S. F. Chen, C. M. Giachelli, B. D. Ratner, and S. Y. Jiang, *J. Biomed. Mater. Res. Part A* **74A**, 23 (2005).

¹⁷Y. Chen, B. S. Bal, and J. P. Gorski, *J. Biol. Chem.* **267**, 24871 (1992).

¹⁸S. M. Martin, R. Ganapathy, T. K. Kim, D. Leach-Scampavia, C. M. Giachelli, and B. D. Ratner, *J. Biomed. Mater. Res. Part A* **67A**, 334 (2003).

¹⁹F. Higashikawa, A. Eboshida, and Y. Yokosaki, *FEBS Lett.* **581**, 2697 (2007).

²⁰E. S. Sorensen and T. E. Petersen, *J. Dairy Res.* **60**, 189 (1993).

²¹A. Krozer and M. Rodahl, *J. Vac. Sci. Technol. A* **15**, 1704 (1997).

²²See EPAPS Document No. E-BJIJOBN-4-002903 for available material on the adsorption of OPN of different concentrations to amine-terminated surfaces, QCM-D raw data, the data in Fig. 4(a) in original form prior to baseline correction and XPS atomic concentration data for the SAMs. For more information on EPAPS, see <http://www.aip.org/Pubserv/epaps.html>.

²³M. L. Wallwork, D. A. Smith, J. Zhang, J. Kirkham, and C. Robinson, *Langmuir* **17**, 1126 (2001).

²⁴M. Rodahl, F. Hook, C. Fredriksson, C. A. Keller, A. Krozer, P. Brzezinski, M. Voinova, and B. Kasemo, *Faraday Discuss.* **107**, 229 (1997).

²⁵G. Sauerbrey, *Z. Physiother.* **155**, 206 (1959).

²⁶E. Stenberg, B. Persson, H. Roos, and C. Urbaniczky, *J. Colloid Interface Sci.* **143**, 513 (1991).

²⁷G. D. Ruxton, *Behav. Ecol.* **17**, 688 (2006).

²⁸E. Reimhult, C. Larsson, B. Kasemo, and F. Höök, *Anal. Chem.* **76**, 7211 (2004).

²⁹J. Malmstrom, H. Agheli, P. Kingshott, and D. S. Sutherland, *Langmuir* **23**, 9760 (2007).

³⁰I. Lundstrom, *Biosens. Bioelectron.* **9**, 725 (1994).

³¹F. Caruso, K. Niikura, D. N. Furlong, and Y. Okahata, *Langmuir* **13**, 3422 (1997).

³²C. Larsson, M. Rodahl, and F. Hook, *Anal. Chem.* **75**, 5080 (2003).

³³C. Zhou *et al.*, *Langmuir* **20**, 5870 (2004)

³⁴M. B. Hovgaard, K. Rechendorff, J. Chevallier, M. Foss, and F. Besenbacher, *J. Phys. Chem. B* **112**, 8241 (2008).

³⁵P. Bingen, G. Wang, N. F. Steinmetz, M. Rodahl, and R. P. Richter, *Anal. Chem.* **80**, 8880 (2008).

³⁶D. G. Castner and B. D. Ratner, *Surf. Sci.* **500**, 28 (2002).

³⁷L. Addadi, N. Rubin, L. Scheffer, and R. Ziblat, *Acc. Chem. Res.* **41**, 254 (2008).